

2. Ljungberg, Y. L., Materials selection and design for development of sustainable products. *Mater. Design*, 2007, **28**(2), 466–479.
3. Baldwin, R., Law, M., Allen, G. and Griffiths, L. G., Survey of fire loads in modern office buildings – some preliminary results. *Fire Safety Sci.*, 1970, **808**, 1.
4. Culver, C., Survey results for fire loads and live loads in office buildings. US Dept. of Commerce, National Bureau of Standards, 1976, no. 85.
5. Kumar, S. and Rao, C. K., Fire loads in office buildings. *J. Struct. Engg.*, 1997, **123**(3), 365–368.
6. Barnett, C. R., Pilot fire load survey carried out for the New Zealand Fire Protection Association, MacDonald Barnett Partners, Auckland, 1984.
7. Narayanan, P., Fire severities for structural fire engineering design. *BRANZ*, 1995.
8. Kose, S. A., Motishita, Y., Hagiwara, I. C., Tsukagoshi, I. S., Matsunobu, S. U. and Kawagoe, K. U., Survey of movable fire load in Japanese dwellings. *Fire Safety Sci.*, 1989, **2**, 403–412.
9. Kumar, S. and Rao, C. K., Fire load in residential buildings. *Build. Environ.*, 1995, **30**(2), 299–305.
10. Zalok, E., Validation of methodologies to determine fire load for use in structural fire protection. *Fire Protection Research Foundation*, 2011, 1–65.
11. Bush, B., Anno, G., McCoy, R., Gaj, R. and Small, R. D., Fuel loads in US cities. *Fire Technol.*, 1991, **27**(1), 5–32.
12. Gao, W., Sun, J., Zhang, Y. and Rong, J., Fire load in students' dormitory buildings. *Int. J. Recent Res. Appl. Stud.*, 2013, **14**, 456–463.
13. Zalok, E. and Eduful, J., Assessment of fuel load survey methodologies and its impact on fire load data. *Fire Safety J.*, 2013, **62**(PART C), 299–310.
14. United Nations. The World's Cities in 2016 – Data Booklet (ST/ESA/SER.A/392). World's Cities 2016, 2016.
15. National Fire Protection Association. NFPA 557 Standard for Determination of Fire Loads for Use in Structural Fire Protection Design, 2011.
16. Buchanan, A. H., *Structural Design for Fire Safety*, Wiley, New York, 2001, vol. 273.
17. Issen, L. A., Single-family residential fire and live loads survey. US Department of Commerce, National Bureau of Standards, Washington, DC, 1980.
18. Thauvoye, C. H., Zhao, B., Klein, J. O. and Fontana, M. A., Fire load survey and statistical analysis. *Fire Safety Sci.*, 2008, **9**, 991–1002.
19. Babrauskas, V., Heat Release Rates. The SFPE handbook of fire protection and engineering. National Fire Protection Association, Quincy, MA, 2002.
20. Holman, J. P., *Heat Transfer*, McGraw-Hill Book Company, Southern Methodist University, 1986.
21. Kanury, A. M., *Introduction to Combustion Phenomena*, CRC Press, 1975, vol. 2.
22. EN BS. 1-2: 2002 Eurocode 1: Actions on structures-Part 1-2: General actions – Actions on structures exposed to fire. British Standards, 1991.

Received 18 July 2017; revised accepted 5 April 2018

doi: 10.18520/cs/v115/i2/320-325

Advances in sea surface layer temperature measurements with fast responding thermistor arrays on drifting buoys

R. Srinivasan^{1,2,*}, V. Rajendran², Shijo Zacharia¹ and Tata Sudhakar¹

¹National Institute of Ocean Technology, Ministry of Earth Sciences, Government of India, NIOST Campus, Chennai 600 100, India

²Vels University, School of Engineering, Electronics and Communication Engineering Department, Pallavaram, Chennai 600 117, India

A precise and accurate ocean temperature measurement system is essential for better understanding and knowledge of the spatial and temporal variability of thermal stratification of the upper-ocean layers is fundamental. The National Institute of Ocean Technology, Chennai has indigenously developed a novel negative temperature coefficient (NTC) thermistor based sensor array with RS232 digital output for drifting buoy (Pradyu) (DB) wherein, it is mainly used in ocean observation applications. The DB is built with Indian satellite (INSAT) for real time data telemetry.

The NTC sensing element is used in developing the temperature sensor for the measurement of sea surface layer temperature. The Steinhart–Hart equation and coefficients are applied on each sampling to zero down the error components involved in temperature measurements which corresponds to the nonlinear functionality of the NTC element. In-house developed SST sensor and sensor array are calibrated and extensively tested in laboratory conditions. The results of the SST and sensor array laboratory calibrations and field validations are briefly presented here with significant data sets collected in the Bay of Bengal warm pool regions.

Keywords: Drifting buoy, NTC thermistor sensor, sensor array, Steinhart–Hart coefficients.

THE sea surface temperature (SST) measured with satellite remote sensing radiometers, ships¹, moored buoys and drifting buoys² has made a major contribution to climate research. Remote sensing of SST is limited by the presence of cloud and rain. The SST products are extensively used in ocean analysis and prediction systems to study the upper-ocean circulation and thermal structure. The SST is an important parameter in oceanographic and atmospheric study and in monitoring of biological habitations. Absolute values of SST are important to understand the nonlinear relationship between atmospheric convection and ocean–atmosphere coupling³. The physical parameters of ocean temperature and conductivity differ in

*For correspondence. (e-mail: rsrini@niot.res.in)

Table 1. SST measurement methods

Method	Sensor	Depth	Resolution	Accuracy	Advantage	Limitations
Ship Bucket ²⁴	Thermometer	Up to 250 m	0.1°C	0.1°C		Dependency on ship voyage
Ship intake ²⁴	Glass thermometer	3 m	0.1°C	0.1°C	Less accurate	Sensor maintenance difficult
Moored buoy ²⁵	RTD	1 m	0.1°C	1°C	Longer period data availability ensured	Not accurate
Drifting buoys ²⁶	RTD/thermometers and Wafer thermistors	~0.16 m	0.1°C	0.1°C/0.5°C	Highly sensitive Excellent repeatability and long-term stability	Endurance of 2 to 3 years at present
ARGO Float ^{27,28}	SBE 41CP	5 m to 2000 m	0.001°C	0.0001°C	Temperature profile application	Temperature measurement up to 5 m surface is not possible
CTD casting ²⁹	Sontek CTD profiler	Up to 100 m	0.01°C	0.05°C	Accurate	Human intervention is required
MBT ³⁰	Liquid in metal thermometers	300 m	0.1°C	0.1°C	Thermal chart based	Not accurate
XBT ¹⁰	RTD	500 to 1800 m	0.1°C	0.1°C	Less sensitive to change in temperature	Linear measurement
Satellite IR ^{26,27}	Infrared sensors	1 μm to 20 μm	1 km coverage	> °C due to regional, seasonal bias and atmospheric effects	Wide coverage	Uncertainty is huge in measurement
Satellite MW ^{26,27}	Microwave transmitters	Near surface	1 km coverage		Wide coverage	Precise measurement is not possible Cloud restricts the overall grid coverage

the Bay of Bengal (BoB) and the Arabian Sea (AS). BoB is low saline and forms strong vertical density stratification due to large inputs of freshwater through precipitation and river discharge⁴. However, AS is highly salty due to the influence of the three major water masses in the northern side, namely the Arabian Sea High Salinity Water (ASHSW) which is generally present in the upper layer of 100 m, Persian Gulf Water mass (PGW) between 200 and 250 m, and Red Sea Water (RSW) between 600 and 900 m (ref. 5). The Lagrangian drifting floats are widely deployed to measure SST and near-surface ocean currents^{6,7}. The technological advances helped develop smart *in situ* sensors for measurement of sea surface and subsurface layer temperatures up to few 100 m depth. Over 20,000 drifting buoys have been deployed globally since 1979, most of them with temperature sensors just below the water line⁸. The various SST measurement methods are listed in Table 1. As the first step we present the underwater sensor architecture, the construction, calibration and its performance evaluation up to 15 m water depth. For better understanding of the temperature characteristics of the ocean, temperature is measured in international temperature scale established during 1990 (ITS-90) in degrees celsius (°C). It is an instrument calibration standard, which provides for comparison and compatibility of temperature measurements internationally for the ocean temperatures typically in the range from

-2°C to 35°C (28.4–95.0°F)⁹. This study focuses on demonstrating the effectiveness of a novel high spatial and temporal resolution temperature sensor array on a drifting buoy developed at the National Institute of Ocean Technology (NIOT), Chennai and comparing the error components involved in different SST observation systems.

The Global Ocean Observation System has defined a program to deploy and maintain 1250 drifting buoys¹⁰ over international water boundaries. NIOT developed drifting buoys with Negative Temperature Coefficient (NTC) thermistors^{11,12}. Internationally drifting buoy producers use different types of temperature sensors to measure SST. Market available drifting buoys are compared in Table 2.

This communication describes the design details of a thermistor sensor array for SST measurements in drifting buoys. Initial set of results from the deployment of the drifting buoy with indigenized thermistor array from 21 March to 26 April 2017 in the Arabian Sea are also presented here.

The drifting buoy is made of a flanged two-part spherical float of 0.4 m diameter made of epoxy resins. The bottom half of the float houses a battery-pack, an embedded system, a power control switch, power control circuits and a satellite modem. The drifting buoy is instrumented with an SST sensor on the bottom half of the hull at 0.16 m below water level and a GPS. The

Table 2. Comparison of Pradyu with available drifting buoys in the market

Specifications	Drifting Buoy (Pradyu) ¹¹	Marlin-Yug ³¹	Metocean ³²
Basic sensor	NTC thermistor element, model YSI 46000 series	Digital thermometer, model- DS18B20 type	Wafer thermistor, model-WM 103
Operating temperature range	-10 to 70°C	-5 to 35.88°C	-2 to 45°C
SST calibrated range	25 to 35°C	-5 to 35.88°C	-2 to 45°C
Accuracy	±0.05°C (25 to 35°C)	±0.1°C (-10 to 85°C)	±0.2°C at 25°C (-0 to 70°C)
Time constant	2.5 sec	120 sec	10 sec
Sensitivity	Higher	Nominal	Higher
Advanced electronics	24 bit ADC is used for digitization Excitation current is measured <i>in situ</i> for each measurements	12 bit ADC is used for digitization	Not available
Best Interchangeability of sensor	±0.05°C (0 to 70°C)	±0.5°C (-10 to 70°C)	±0.4°C @35°C

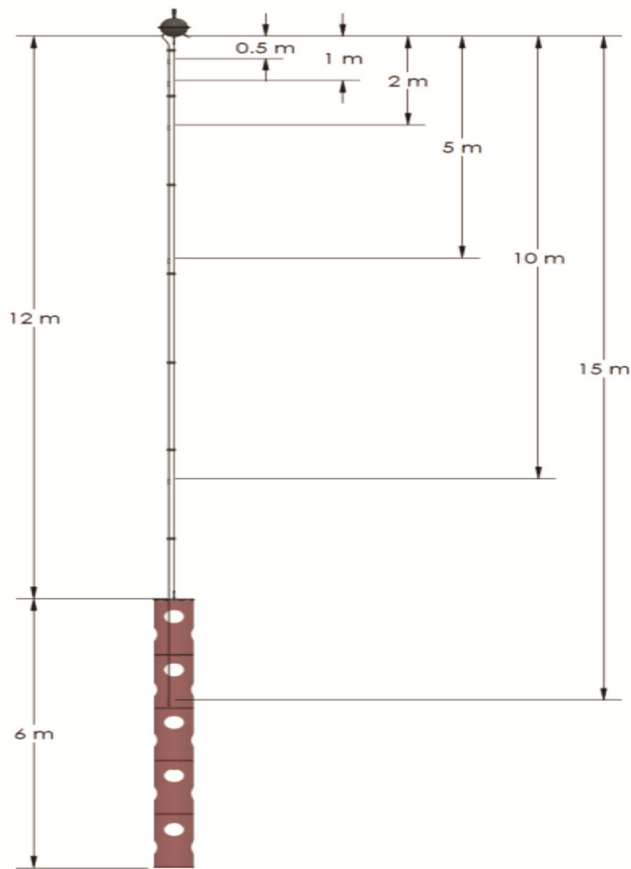


Figure 1. Drifting buoy with subsurface temperature scheme complete view (NTC thermistor temperature capsules at 0.5 m, 1 m, 2 m, 5 m, 10 m and depth sensor capsule at 15 m).

bottom half of the sphere is coated with antifouling paint. The upper half of the float is coated with ultraviolet protective coating. A plastic impregnated stainless steel wire of length 12 m and diameter 3.2×10^{-3} m is connected to an eye bolt at the bottom centre of the float. The bottom centre of the float is strengthened internally. The bottom end of the tether is attached to a disc type frame on a windowed cylindrical holy sock drogue. The drogue has PVC ribs to keep it circular.

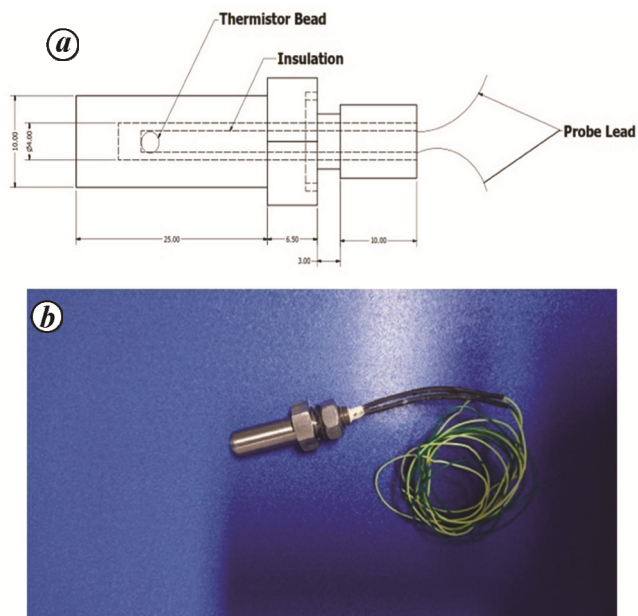


Figure 2. *a*, TS1 probe drawing (dimensions in mm); *b*, image of NTC thermistor (SST sensor).

The thermistor array has six underwater temperature sensors encapsulated with thermally conductive epoxy resin. The temperature sensors are deployed at 0.16 m (TS1), 0.5 m (TS2), 1 m (TS3), 2 m (TS4), 5 m (TS5), 10 m (TS6) and 15 m (TS7) and also one depth sensor deployed at 15 m (Figure 1). A high precision and fast responding NTC thermistor element (YSI 46000 series)¹³ is employed as a temperature sensor at these depths. A reference resistor method is adopted to make the measurement independent of offset error. In this method, a current source excites a NTC thermistor sensor (YSI 46000). The voltage across the NTC thermistor which varies in proportion to the temperature is accurately measured. ITS-90 temperature measurement standards are followed for sensor array design and temperature measurements. The NTC thermistor at 0.16 m depth is sealed in the bore hole of a stainless steel rod with thermally

conductive potting compound ER2074 (ref. 14). The thermistor mounting, thermally isolated from the inside of the float, is designed to react quickly to changes in SST. Thermal isolation prevents solar heating of the top of the surface float from influencing the SST measurements¹⁵. The drawing and image of the SST probe are shown in Figure 2 *a* and *b* respectively. It is thermally isolated internally with foam and mounted in the hull. The pictorial view of the SST sensor mounted in the buoy at 0.16 m depth is shown in Figure 3. A low power processor interfaced with a data acquisition board digitizes the amplified voltage signals with 24-bit resolution. The module at 15 m depth has a pressure sensor to measure the depth. A low power processor interfaced with the data acquisition board digitizes the amplified voltage signals with 24-bit resolution. The photograph of the thermistor sensor array is shown in Figure 4. The data acquisition is made of a low power, reconfigurable, programmable system on chip PSOC manufactured by Cypress semiconductor, USA¹⁶. The nonlinearity of the thermistor sensors is corrected with Stein–Hart and Hart model and calibration coefficients¹⁷.

A DB (P25) is interfaced with the thermistor string which profiles temperature (TS_1–TS_6) at 0.5 m, 1 m,



Figure 3. SST sensor in drifting buoy.

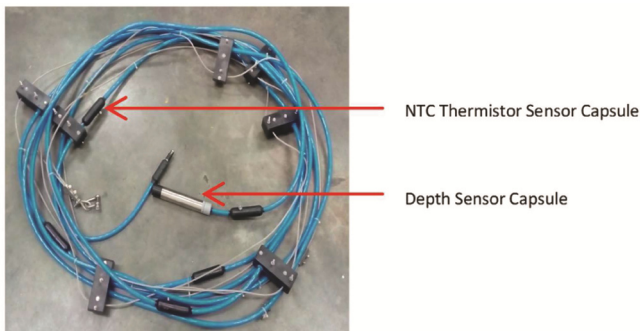


Figure 4. Temperature sensor array.

2 m, 5 m, 10 m and 15 m mixed layer water depth. Profile depth is ensured by a pressure sensor at the bottom most section of the string.

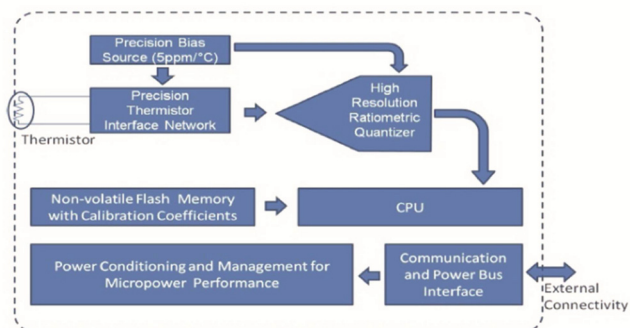


Figure 5. Electrical design architecture of the temperature sensor.

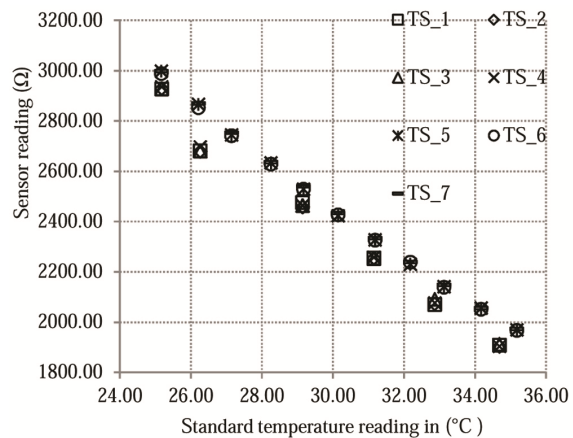


Figure 6. Temperature response of sensors.

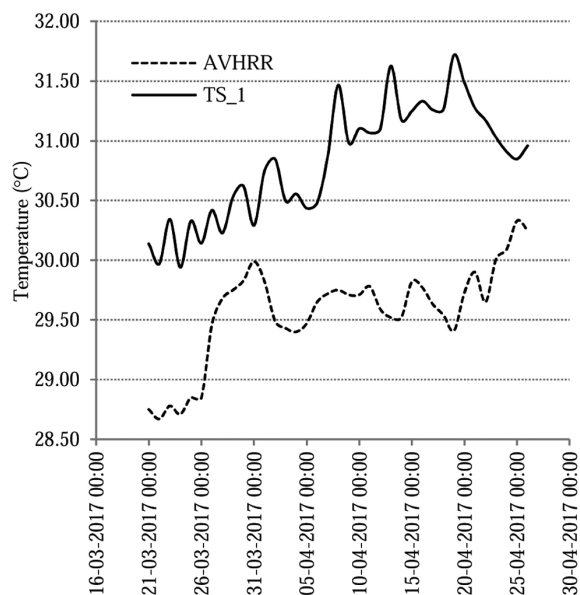


Figure 7. The daily mean of SST measured by drifting buoy and AVHRR.

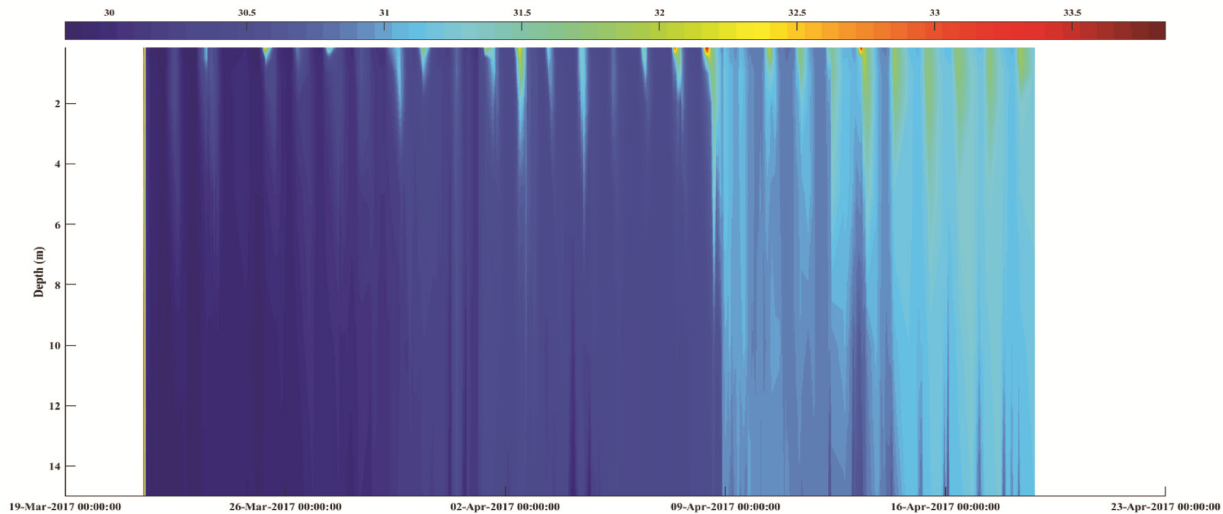


Figure 8. Vertical section temperature.

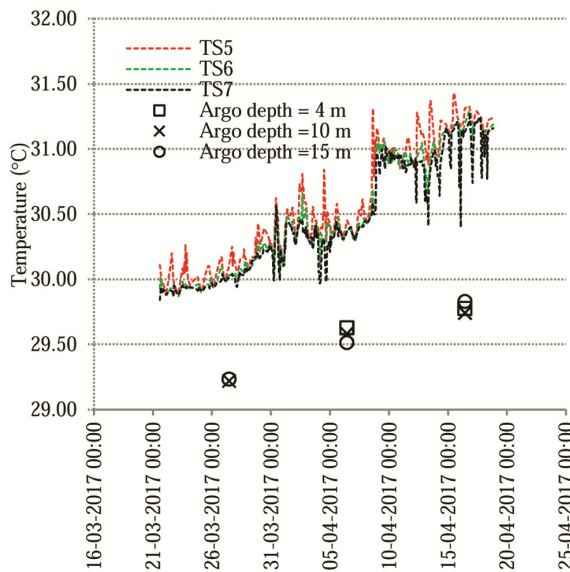


Figure 9. The vertical profiles of temperature measured by drifting buoy and Argo.

The thermistor has a nonlinear resistance change-over temperature. Although the thermistor is nonlinear, it can be tamed for a limited temperature range. This allows the design of an inexpensive temperature sensing device. The SST sensor is calibrated for 25–35°C temperature range at National Accreditation Board for Laboratories accredited calibration facility and accuracy verified with 5 point calibration (Figure 5). The master reference has an expanded uncertainty of $\pm 0.02^\circ\text{C}$ (resistance temperature detectors) and $\pm 0.004\%$ (digital multimeter) on resistance measurements. These reference calibration systems are traceable to the National Institute of Standards and Technology. The temperature sensors response at various temperatures from 25.17°C to 36.18°C is shown in Figure 6. The temperature resistance response of the sensor is

approximated in the range of 25 – 30°C with a third order polynomial curve fitting method.

A GPS receiver module with 65 channels at L1 frequency of 1575.42 MHz coarse acquisition code provides positional information and time synchronization. The GPS has circular error probability of 2.5 m radius. The GPS receiver is normally in ‘off’ state and is switched on for 60 sec and position is captured in the next 60 sec. The power to the GPS is switched off after position and time acquisition. The GPS module is interfaced to the controller module through RS232 TTL interface in National Marine Electronic Association, 4800 bits per second protocol.

The temperature sensor array measures the water column temperature at every minute. The measurement is averaged at 15 min interval. The measured data is stored in an onboard memory. The system measures position data from the GPS. The system transmits averaged temperature data and position through satellite telemetry after encoding.

The ocean research vessel, *Sagar Manjusha* deployed the indigenized drifting buoy with NTC thermistor sensor array at position 8.5°N and 70.0°E on 21 March 2017. The drifting buoy collected the SST profile data for about a month, i.e. 21 March to 26 April in 2017 in the Arabian Sea.

The daily mean of SST from AVHRR data over the region from 21 March to 26 April 2017 were analysed and results were compared¹⁸ (Figure 7).

Vertical profiles of temperature from the Argo float^{19–21} on 27 March, 6 and 16 April 2017 (Figure 8) were compared with the drifting buoy data. The Argo float was away from drifting buoy on 27 March, 6 and 16 April 2017 by 204 km, 203 km and 168 km respectively.

The SST profile measured by the drifting buoy in the Arabian Sea from 21 March to 11 April 2017 is shown in Figure 7. A warming of the ocean from 29.85°C to 31.12°C is observed in the SST (SST1). The warming of the ocean active layer is also distinct in this period. The

diurnal amplitude of the SST extended beyond the measuring range in April.

The daily mean of SST measured by the drifting buoy and AVHRR is shown in Figure 7. The AVHRR SST measurements also show the warming of the ocean by about 1.66°C. The SST in AVHRR corresponds to the top 10 µm or so, whereas the SST (TS1) in the measurement is at 0.16 m depth. The difference between the above measurements could be partly due to difference in sensing depth, regional and seasonal bias and atmospheric effects^{18,22,23}.

The drifting buoy measured temperature (T) depth profiles up to 15 m depth. The vertical profiles of temperature measured by the drifting buoy and Argo were compared (Figure 9). The Argo temperature measurements also show the warming of the Ocean by about 0.598°C. The drifting measurements are higher by about 0.5°C. These discrepancies are due to spatial and temporal differences.

In this study we have presented the effectiveness of an indigenized drifting buoy and sensor array for real time monitoring of the ocean active layer. The design details of the temperature sensor array and calibration methods of the drifting buoy are reported here. The developed drifting buoy was tested in the Arabian Sea from 27 March 2017 to 18 April 2017. The warming of the ocean by about 1.27°C was observed in the drifting buoy data. The results were compared with AVHRR and Argo data. The Argo temperature profile and AVHRR SST measurements also showed the warming of the Ocean by about 0.598°C and 1.66°C respectively. The high resolution *in situ* SST measurements by drifting buoys were used for comparing and validating satellite based SST data. The temperature sensor array has wide application with data buoys.

More sensors are required to monitor the ocean active layer with high SST resolution of 10 km globally and 1 km regionally as recommended by DBCP.

1. Kent, E., Ball, G., Berry, D., Fletcher, J., North, S. and Woodruff, S., The Voluntary Observing Ship (VOS) Scheme. In Proceedings of OceanObs'09: Sustained Ocean Observations and Information for Society Conference, Venice, Italy, 2009, ESA Publication WPP-306, doi:10.5270/OceanObs09.cwp.48.
2. Tabata, S., An evaluation of the quality of sea surface temperatures and salinities measured at station P and line P in the Northeast Pacific Ocean. *J. Am. Meteorol. Soc.*, 1968, **8**, 970–986.
3. Bjerknes, J., Atmospheric teleconnections from the equatorial Pacific. *J. Am. Meteorol. Soc.*, 1969, **97**, 163–172.
4. Shenoi, S. S. C., Shankar, D. and Shetye, S. R., Differences in heat budgets of the near surface Arabian Sea and Bay of Bengal: Implications for the summer monsoon. *J. Geophys. Res.*, 2002, **107(C6)**, 5-1–5-14.
5. Prasanna Kumar and Prasad, T. G., Formation and spreading of Arabian Sea high salinity water mass. *J. Geophys. Res.*, 1999, **104(C1)**, 1455–1464.
6. Smith, P., Frye, D. and Cresswell, G., New low-cost ARGOS drifting buoy. Oceans Conference, Washington DC, USA, 1984, pp. 745–747; doi:10.1109/OCEANS.1984.1152276.

7. Lanza, M., A low-cost expendable Loran-based drifting buoy. Oceans Conference, Washington DC, USA, 1984, pp. 741–744; doi:10.1109/OCEANS.1984.1152286.
8. Luca centurioni, Lance braasch., Verenna harmann., The global drifter program observations of sea surface temperature in the world's ocean. DBCP report 2016.
9. Talley, L. D., *Descriptive Physical Oceanography – An Introduction*, 2011, 6th edn.
10. www.aoml.noaa.gov/phod/dac/GDP_2010-2.pdf
11. Shijo Zacharia, Seshasayanan, R., Srinivasan, R., Thamarai, T., Tata Sudhakar, Rao, R. R. and Atmanand, M. A., Design, development and validation of smart sensor drifting node with INSAT telemetry for oceanographic applications. *Curr. Sci.*, 2014, **106**(6), 831–840.
12. Srinivasan, R., Zacharia, S., Sudhakar, T., Thamarai, T., Gowthaman, V. and Atmanand, M. A., A smart sensor drifting buoy node with INSAT communication for meteorological and oceanographic applications. Indian Patent Office, 16/08. 2013, p. 20633.
13. YSI Precision Thermistors & Probes, www.ySI.com.
14. http://www.electrolube.com/core/components/products/tds/044/ER_2074.pdf (accessed on 15 January 2011).
15. Sybrandy, A. L., Neiler, P. P., Martin, C., Scuba, W., Char pentier, E. and Meldrum, D. T., DBCP Report No.4, on Global Drifter Program-Barometer drifter design reference, Data buoy cooperation panel, 2009.
16. <http://www.cypress.com/psoc> (accessed on 15 August 2013).
17. Steinhart, J. S. and Hart, S. R., Calibration curves for thermistors, *Deep-Sea Res. Oceanogr. Abstr.*, 1968, **15**(4), 497–503; ISSN 0011-7471.
18. <http://las.incois.gov.in/> (accessed on 6 February 2017).
19. http://www.argo.ucsd.edu/Argo_GE.html (accessed on 6 February 2017).
20. Boyer, T. P. et al., World Ocean Database 2013. Sydney Levitus, Ed.; Alexey Mishonov, Technical Ed.; NOAA Atlas NESDIS 72, 2013, p. 209.
21. http://ftp.seabird.com/products/spec_sheets/41data.html (accessed on 6 February 2017).
22. Wentz, F. J., Gentemann, C., Smith, D. and Chelton, D., Satellite measurements of sea surface temperature through clouds. *Science*, 2000, **288**, 847–850.
23. Park, K.-A., Lee, E.-Y., Chung, S.-R. and Sohn, E.-H., *Korean J. Remote Sensing*, 2011, **27**(6), 663–675.
24. <http://www.ndbc.noaa.gov>
25. O'Carroll, A. G., Eyre, J. R. and Saunders, R. W., Three way error analysis between AATSR, AMSR-E, and In Situ Sea surface temperature observations. *J. Atmos. Ocean Technol.*, 2008, **25**, 1197–1207.
26. <http://www.argo.ucsd.edu> (accessed on 11 May 2017).
27. [ftp://ftp.wmo.int/Documents/PublicWeb/amp/mmop/documents/dbcp](http://ftp.wmo.int/Documents/PublicWeb/amp/mmop/documents/dbcp)
28. <http://www.argo.ucsd.edu> (accessed on 17 May 2017).
29. <http://www.sontek.com> (accessed on 11 March 2016).
30. Thomson, R. E. and Emery, W. J., *Data Analysis Methods in Physical Oceanography*, Elsevier and Book Aid International, 2014, 3rd edn.
31. <http://www.marlin-yug.com> (accessed on 30 January 2013).
32. <http://www.metcean.com> (accessed on 17 June 2016).

ACKNOWLEDGEMENTS. We acknowledge the Ministry of Earth Sciences, Government of India for funding this research. We also acknowledge the active support of the Ocean Electronic Department, NIOT for deployment operations. We thank Indian National Centre for Ocean Information Services (INCOIS), Hyderabad, for providing data from buoy, AVHRR and Argo data service in live access server.

Received 30 May 2017; revised accepted 28 February 2018

doi: 10.18520/cs/v115/i2/325-330